ELSEVIER

Physica C 277 (1997) 24–35

PHYSICA C

Optimized synthesis and properties of chemically stabilized $CuSr_2YCu_2O_7$

B. Dabrowski [*,a], K. Rogacki [a], J.W. Koenitzer [b], K.R. Poeppelmeier [b], J.D. Jorgensen [c]

[a] *Physics Department, Northern Illinois University, DeKalb, IL 60115, USA*
[b] *Department of Chemistry, Northwestern University, Evanston, IL 60208, USA*
[c] *Materials Science Division, Argonne National Laboratory, Argonne, IL 60439, USA*

Received 7 November 1996

Abstract

Synthesis of the $CuSr_2YCu_2O_7$ compounds with Re, W and Mo substituted for Cu has been optimized for the highest T_c. Materials prepared in air at 990°C and annealed at 650–700°C in 220 atm. O_2 are tetragonal with the transition elements substituting on the Cu-"chain" site, have oxygen content ~ 7.3, and are superconducting with $T_c \sim 70$ K. The irreversibility lines show rather poor pinning characteristics when compared to Y123. Superconducting T_c values were increased up to 77 K by additional substitution of small amounts of Ca for Y. Based on a.c. susceptibility and d.c. magnetization measurements, Ca substitution improves superconducting properties making chemically stabilized $CuSr_2YCu_2O_7$ materials interesting for high field applications below 30 K.

1. Introduction

The Sr-based analog of $YBa_2Cu_3O_7$ can be prepared only at very high oxygen pressures [1,2]. This material contains a single metal–oxygen layer in the blocking layer separating the double CuO_2 planes, and, thus, the chemical formula may be written as $CuSr_2YCu_2O_7$ [3]. Material with strontium replacing barium can be stabilized at atmospheric pressure by the partial or complete substitution for copper in the blocking layer ("chain" site) with small transition or post-transition metals [4,5], large ions, Hg, Tl, Pb, Bi [3,6], mixtures of small and large ions [7] or by partial substitution with lanthanum on the Sr-site [8].

Owing to the ease of preparation in air and the absence of toxic fumes during the synthesis, compounds stabilized with small metal ions, $Cu_{1-x}M_xSr_2RE_{1-y}Ca_yCu_2O_z$ (M = Al, Ga, Fe, Co, Ti, Ge, V, Cr, Mo, W and Re), are of interest [5]. The complete replacement of "chain" copper, $x = 1$, can be achieved for +3 ions, Al, Ga, Fe and Co, for most rare earths and yttrium with the oxygen content, z, close to 7; and for +5 ions, Nb and Ta, for large rare earths with $z \sim 8$ [9]. For compounds with +3 and +5 ions replacing copper on the "chain" site and $x = 1$, superconductivity was achieved only for Ga ($y \sim 0.35$, $T_c \sim 50$–70 K) after a high-pressure oxygen anneal [10]. Substitution of part of the doped ions, Al, Fe and Co, for copper on the plane site is the probable cause of the destruction of superconductivity for compounds substituted with +3

* Corresponding author. Fax: +1 630 252 7777.

PII S0921-4534(97)00044-0

ions [11]. Achieving sufficient hole doping may be the reason for the absence of superconductivity for compounds substituted with +5 ions.

The unwanted substitution for copper on the plane site can be avoided when copper is only partially substituted with small ions ($x < 1$). With the exception of the aluminum and chromium compounds, superconductivity is then obtained in a tetragonal structure and the superconducting T_c can be increased with high-pressure oxygen anneal which increases the oxygen content above 7 [5]. The highest superconducting T_c is observed at a minimum amount of substitution for copper required to form the single-phase material. T_c is related to the formal valence of the substituted ion; the higher valences corresponding to the higher observed T_c values. Since these materials contain smaller strontium in place of a larger barium in the intermediate region, it is expected that the separation between the copper-oxygen planes, owing to the thickness of the intermediate region, should be decreased compared to Y123 and as a result the Sr-based materials may show improved flux pining properties. Thus, the irreversibility fields and critical current behavior of $Cu_{1-x}M_xSr_2YCu_2O_z$ materials stabilized with high valence transition elements for copper are interesting for study. Here, we describe optimized compositions and synthesis conditions for materials with the highest T_c that can be achieved for M = Re, W and Mo. Structural and superconducting properties are described in detail and compared with recently published data for similar materials.

2. Synthesis and characterization

Polycrystalline samples of $Cu_{1-x}M_xSr_2Y_{1-y}Ca_yCu_2O_z$ (M = Mo, W and Re) were synthesized from stoichiometric mixtures of the oxides and carbonates of MoO_3, WO_3, Re_2O_7, Y_2O_3, CuO, and $SrCO_3$ and $CaCO_3$ then fired in air followed by fast cooling to room temperature. Samples were heated for several days with frequent intermediate grindings. The high pressure annealings were done for 12 hours in 20% O_2 in argon at a total pressure of 3 kbar (600 atm O_2 pressure) at 950–100°C or in pure oxygen (220 atm O_2) at 400–900°C followed by slow cooling (0.2°/min.) to room temperature. Sample homogeneity was checked by powder X-ray diffraction. Neutron powder diffraction data were obtained using the Special Environment Powder Diffractometer (SEPD) [12] at Argonne National Laboratory's Intense Pulsed Neutron Source (IPNS). Susceptibility and magnetization measurements were performed with a Quantum Design Physical Properties Measurement System. Resistivities were measured using the standard four-lead d.c. measurement technique. Oxygen contents were determined by thermogravimetric analysis measurements using a Cahn TG171 system with slow (0.6°/min.) heating and cooling rates.

3. Results and discussion

3.1. Synthesis and T_c

Our goal was to maximize the superconducting T_c by determining the optimum synthesis and annealing conditions of temperature and oxygen pressure. Samples were fired several times at increasing temperatures, checked for phase purity, annealed under several oxygen pressures and temperatures, and T_c measured. In Table 1, the results of various firing steps are presented for $Cu_{0.8}W_{0.2}Sr_2YCu_2O_z$. Samples synthesized in air are single phase for 980–990°C. Multiple-phase samples formed for temperatures lower than 975°C; the amount of impurity phases decreased with increasing temperature. Partial melting and small amounts of impurity phases were observed for temperatures higher than 990°C. High pressure oxygen annealings at temperatures around 650–700°C followed by slow cooling were optimal for increasing the oxygen content and to obtain the highest T_c. At lower temperatures, oxygen diffusion was too slow in the dense pellets, resulting in the lower and broader superconducting transitions. For higher annealing temperatures, a decrease of T_c from the maximum value was probably a result of metal ion disorder, i.e., substitution of part of the W onto the Cu-plane site or Sr onto the Y-site. For the optimized oxygen anneal around 700°C, the best samples were obtained when the first synthesis step was made at 990°C. Synthesis under moderately reduced oxygen pressures (4 and 0.8% O_2 in Ar) did not produce better material. Small amounts of cal-

Table 1
Synthesis conditions and properties of the resulting material for $Cu_{0.8}W_{0.2}Sr_2YCu_2O_z$

Synthesis temperature (°C)	Oxygen anneal	Resulting material, T_c (K)
940	air	multi-phase, semimetalic, 28 K
960	oxygen	multi-phase, semimetalic, 51 K
960	220 atm, 700°C	multi-phase, metalic, 66 K
975	air quenched	almost pure 1212 phase
985	220 atm, 500°C	pure 1212 phase, metalic, 65 K
985	220 atm, 700°C	pure 1212 phase, metalic, 75 K
985	220 atm, 900°C	pure 1212 phase, metalic, 44 K
985	600 atm, 1100°C	pure 1212 phase, metalic, 53 K
990	220 atm, 700°C	pure 1212 phase, metalic, 77 K
1000	220 atm, 700°C	almost pure 1212 phase, metalic, 74 K

cium, less than 10%, can be substituted for yttrium resulting in material with T_c increased from ~ 70 to 77 K. The pure and Ca-doped materials prepared at 990°C followed by 220 atm. O_2 anneal at 700°C were chosen for structural and superconducting characterization, respectively.

Similar results were obtained for M = Re (x = 0.15) and Mo (x = 0.2). Samples prepared at 990°C followed by 220 atm. O_2 anneal at 700°C were chosen for further characterization. Fig. 1a shows normalized resistivities for the best single phase samples that were obtained with substitution of transition metals only. Fig. 1b shows normalized resistivities for the almost single-phase samples synthesized with the additional substitution of 10% Ca for Y. In both cases, the highest T_c values were obtained for materials stabilized with W. The superconducting transitions are sharp indicating good sample quality. The measured T_c are the highest ever reported for the Sr based 1212 structure stabilized by small transition metal ions. All samples annealed at high oxygen pressure show metallic resistivities while samples prepared in air show nonmetallic behavior. The ac susceptibility data for the powdered $Cu_{0.8}W_{0.2}Sr_2YCu_2O_z$ sample substituted with Ca is shown in Fig. 1b. Susceptibility measurements for other samples substituted with Mo and Re showed similar, reasonably sharp transitions.

3.2. Structure and oxygen content

The powder neutron-diffraction data were collected for ~ 3 g samples at room temperature. Rietveld structural refinements were carried out using the GSAS code [13] over the range $0.5 < d < 4.0$ Å. For each pattern, 17 structural parameters were refined. The observed and calculated patterns for the three samples are shown in Figs. 2a–c. The patterns were indexed using a tetragonal cell, space group P4/mmm. The initial model used for our refinements was based on the structure proposed by Harlow et al. [14] in which the chain site $(Cu,M)O_6$ octahedra are rotated. As a consequence of the rotation, chain oxygens O(1) are displaced from the mirror site (0, 0.5, 0) to an off-mirror site (x, 0.5, 0). Using this model, a significant residual was seen in the Fourier difference map on the (0, 0.05, 0) site; therefore, a split chain oxygen O(1) position, consisting of (0, 0.5, 0) and (x, 0.5, 0) sites was employed in our refinements. In addition, a model proposed by Slater and Greaves [15] in which the O(1) chain oxygen is split into two off-mirror positions ($x1$, 0.5, 0) and ($x2$, 0.5, 0) was tested. By using two off-mirror oxygens, the refinement statistics improved slightly, R_{wp} was reduced from 0.0581 to 0.0575 and the χ^2 from 1.710 to 1.676; however, the thermal parameters of the O(1a) and O(1b) given in units of $100 \times U_{iso}$ (Å^2) increased from 1.43 to 2.05 and from 2.54 to 6.08, respectively. As a result, we chose to model the structures with a split O(1) position consisting of a mirror-site (0, 0.5, 0) and off-mirror site (x, 0.5, 0). The substituted cation M was found to occupy solely the chain site. The refined structural parameters and selected bond angles and distances are given in Tables 2 and 3.

The oxygen stoichiometries of the samples were obtained from the oxygen occupancies. Initially, the O(2) and O(3) occupancies refined to approximately

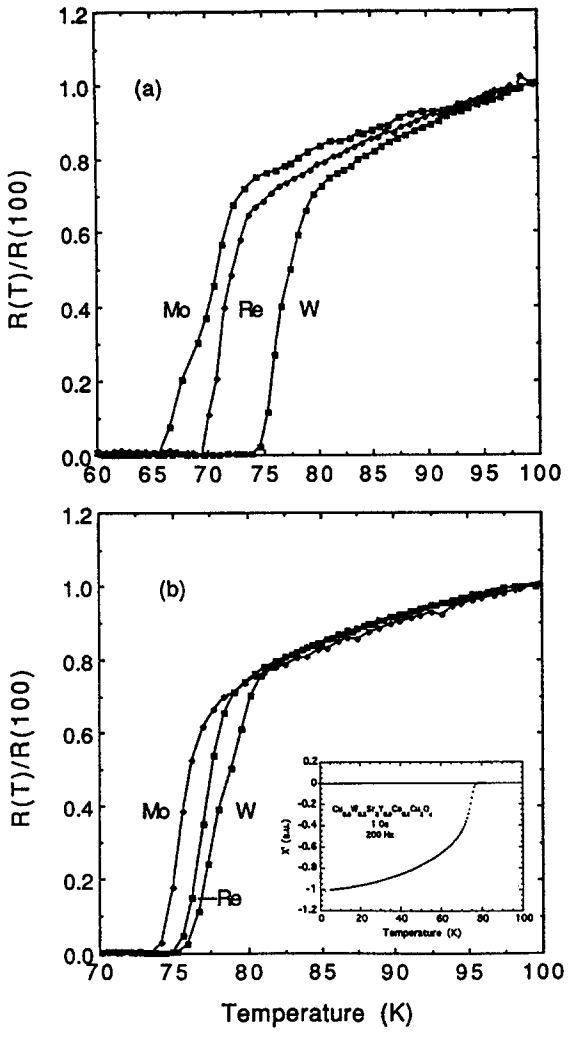

Fig. 1. Normalized resistances for $Cu_{1-x}M_xSr_2YCu_2O_z$ samples with substitution of (a) transition metals, and (b) with the additional substitution of 10% calcium for yttrium. Inset shows a.c. susceptibility for a powdered $Cu_{0.8}W_{0.2}Sr_2YCu_2O_z$ sample substituted with calcium.

1.0. Consequently, they were set to 1.0 and not refined. The oxygen stoichiometries as determined by neutron diffraction and valance calculations (in brackets) are 7.30 (7.28), 7.30 (7.30) and 7.30 (7.29) for Mo, W and Re, respectively. The refined oxygen stoichiometries are approximately equal to the oxygen contents found by replacing chain Cu^{3+} with M cations in their highest allowed oxidation states consistent with the preparation conditions (Mo^{6+}, W^{6+}, and Re^{7+}). For Mo and W substitutions, the maximum observed T_c occurred at doping levels of $x = 0.20$ and an oxygen content of 7.30 while for Re substitution T_c maximum occurred at a doping level of $x = 0.15$ and an oxygen content of 7.30. Therefore, three oxide anions are added to the chain layer for every 2 Mo or W cations substituted, while two oxide anions are added for every Re cation.

Since the substituted cations exist in an octahedral environment in the chain layer, the following model is proposed to account for the observed oxygen stoichiometries. In the case of Mo and W, randomly distributed dimmers of corner shared octahedra would give the observed 2/3 (Mo, W)/O ratio, while, in the Re sample, isolated Re octahedra are consistent with the observed 1/2 Re/O ratio. The model structures compared to 123 are shown in Fig. 3.

The schematic picture representing similar two-CuO_2-planes compounds with a single metal-oxygen layer in the intermediate region is shown in Fig. 4. The important distances are the inter-CuO_2-plane, d(inter), which defines the thickness of the intermediate region and the intra-CuO_2-plane, d(intra). The sum of these two distances is equal to the c axis lattice constant. The thickness of the intermediate region consists of a sum of two distances, twice the apical bond length of the planar copper, d(apical), and d(block) which is defined as twice the $Cu/M(1)$-O(2) bond length. The d(block) is the thickness of the blocking layer where transition and post-transition metals are substituted for copper. This region strongly affects the c-axis normal state and superconducting properties. The relevant distances and superconducting T_c are given in Table 4 for three optimally doped compounds, $CuBa_2YCu_2O_7$ (Y123), $Cu_{0.8}W_{0.2}Sr_2YCu_2O_{7.3}$ and $HgBa_2CaCu_2O_6$. The large variations of T_c can be explained by the apical bond-length of the planar copper, d(apical) [16,17]. The long bond enhances the two-dimensional features of the electronic structure through removal of the e_g $3d_{z^2-r^2}$ orbitals below the Fermi surface owing to the increased Jahn-Teller distortion. The enhanced two-dimensional features, for example, Van Hove singularities of electronic density of states, favor higher superconducting transition temperatures. The $Cu_{0.8}W_{0.2}Sr_2YCu_2O_{7.3}$ compound has the shortest d(apical) and, thus, the lowest T_c. As expected, the thickness of the intermediate region is the shortest for the Sr-based material. This is due to

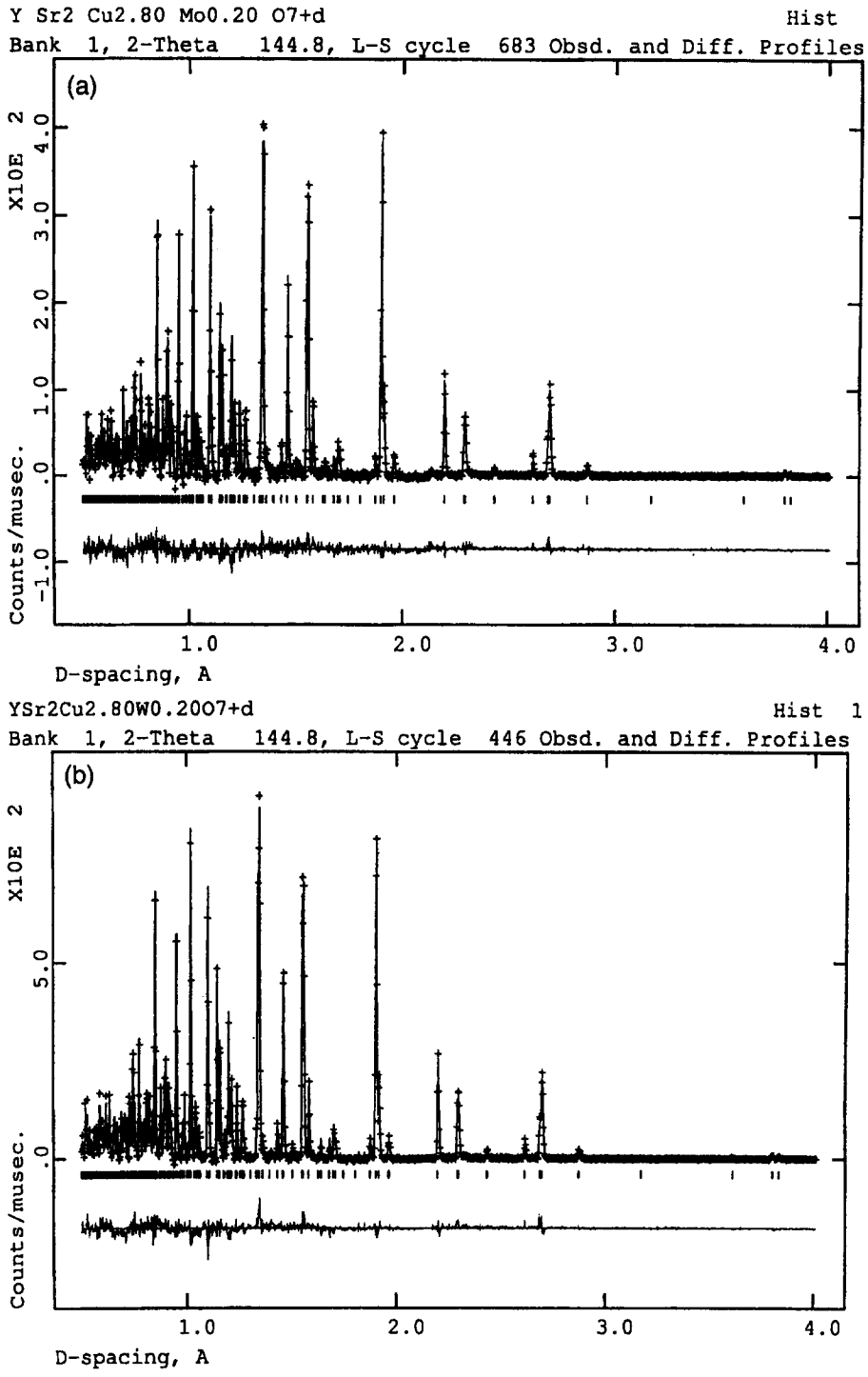

Fig. 2. Part of the observed and calculated neutron diffraction patterns for the $Cu_{1-x}M_xSr_2YCu_2O_z$ samples, (a) M = Mo, (b) M = W and (c) M = Re.

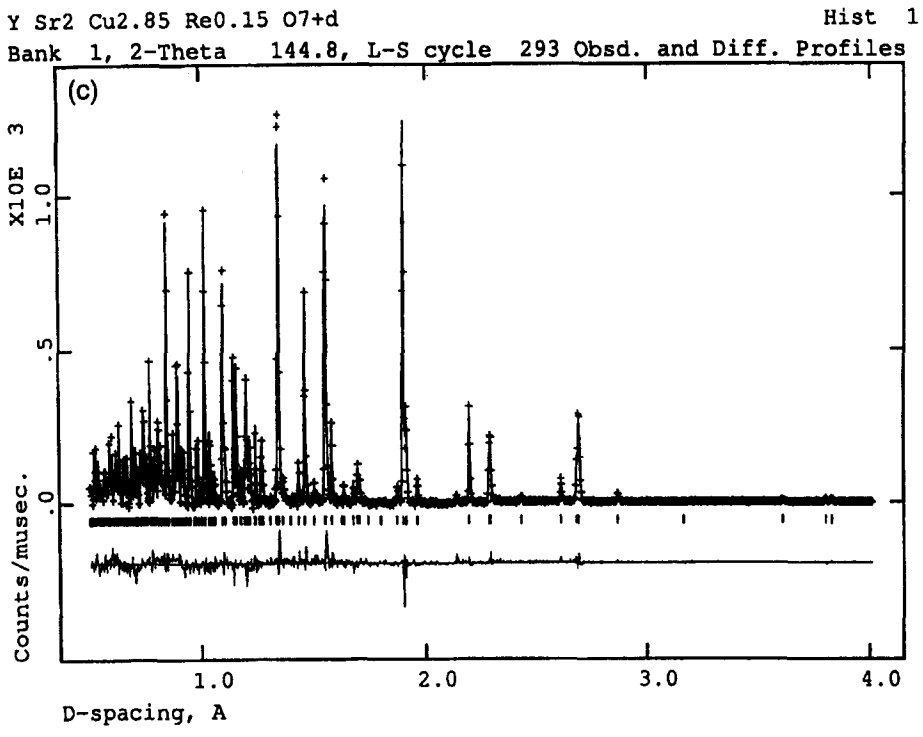

Fig. 2 (continued).

both, the shorter d(apical) and a slightly shorter thickness of the blocking layer.

The refinements clearly show more than seven oxygen atoms per unit cell. This is in qualitative agreement with TGA measurements. Clearly, the presence of high valence transition metals draws additional oxygen into the structure. The $Cu_{0.8}W_{0.2}Sr_2YCu_2O_z$ sample annealed at 220 atm. O_2 was chosen for a detailed characterization of the oxygen content vs temperature and oxygen partial pressure using thermogravimetric measurements. To assure quasi-equilibrium conditions, the thermogravimetric

Table 2a
Refined structural parameters for $Cu_{0.80}Mo_{0.20}Sr_2YCu_2O_{7+d}$ at room temperature. Space group P4/mmm. Lattice constants are $a = 3.8013(1)$ and $c = 11.4861(3)$. Cell volume = 165.971(5). Powder data statistics: $R_{wp} = 0.0796$, $R_p = 0.0489$, $R_F^2 = 0.0988$, $\chi^2 = 1.372$ for 29 variables, $N_{obs} = 501$

Atom	Site	x	y	z	$100 \times U_{iso}$ (Å^2)	Occupancy
Y	1d	0.5	0.5	0.5	0.46(6)	1.0
Sr	2h	0.5	0.5	0.1876(2)	1.82(7)	1.0
Cu(1)	1a	0.0	0.0	0.0	1.55(8)	0.8
Mo	1a	0.0	0.0	0.0	1.55(8)	0.2
Cu(2)	2g	0.0	0.0	0.3530(2)	0.56(5)	1.0
O(1a)	2f	0.0	0.5	0.0	1.74(95)	0.146(32)
O(1b)	4n	0.161(5)	0.5	0.0	2.84(46)	0.248(19)
O(2)	2g	0.0	0.0	0.1610(3)	1.78(8)	1.0
O(3)	4i	0.0	0.5	0.3742(2)	0.95(5)	1.0

Table 2b
Refined structural parameters for $Cu_{0.80}W_{0.20}Sr_2YCu_2O_{7+d}$ at room temperature. Space group P4/mmm. Lattice constants are $a = 3.8020(3)$ and $c = 11.4971(2)$. Cell volume = 166.195(3). Powder data statistics: $R_{wp} = 0.0682$, $R_p = 0.0456$, $R_F^2 = 0.1011$, $\chi^2 = 2.218$ for 28 variables, $N_{obs} = 503$

Atom	Site	x	y	z	$100 \times U_{iso}$ (Å^2)	Occupancy
Y	1d	0.5	0.5	0.5	0.71(4)	1.0
Sr	2h	0.5	0.5	0.1877(2)	1.90(5)	1.0
Cu(1)	1a	0.0	0.0	0.0	1.57(6)	0.8
W	1a	0.0	0.0	0.0	1.57(6)	0.2
Cu(2)	2g	0.0	0.0	0.3529(1)	0.63(3)	1.0
O(1a)	2f	0.0	0.5	0.0	0.90(51)	0.147(18)
O(1b)	4n	0.1672(34)	0.5	0.0	3.05(33)	0.252(12)
O(2)	2g	0.0	0.0	0.1612(2)	1.87(6)	1.0
O(3)	4i	0.0	0.5	0.3747(1)	1.09(3)	1.0

Table 2c
Refined structural parameters for $Cu_{0.85}Re_{0.15}Sr_2YCu_2O_{7+d}$ at room temperature. Space group P4/mmm. Lattice constants are $a = 3.7998(4)$ and $c = 11.4748(2)$. Cell volume = 165.706(3). Powder data statistics: $R_{wp} = 0.0581$, $R_p = 0.0384$, $R_F^2 = 0.1022$, $\chi^2 = 1.710$ for 29 variables, $N_{obs} = 500$

Atom	Site	x	y	z	$100 \times U_{iso}$ (Å^2)	Occupancy
Y	1d	0.5	0.5	0.5	0.51(4)	1.0
Sr	2h	0.5	0.5	0.1877(2)	1.88(5)	1.0
Cu(1)	1a	0.0	0.0	0.0	1.42(6)	0.85
Re	1a	0.0	0.0	0.0	1.42(6)	0.15
Cu(2)	2g	0.0	0.0	0.3528(1)	0.51(3)	1.0
O(1a)	2f	0.0	0.5	0.0	1.43(67)	0.138(22)
O(1b)	4n	0.169(4)	0.5	0.0	3.43(38)	0.254(14)
O(2)	2g	0.0	0.0	0.1605(2)	1.69(6)	1.0
O(3)	4i	0.0	0.5	0.3744(1)	0.93(4)	1.0

Table 3
Selected bond distances and angles for the series $Cu_{1-x}M_xSr_2YCu_2O_{7+d}$ with M = Mo, W and Re.

	$Mo_{0.20}$	$W_{0.20}$	$Re_{0.15}$
Cu(1)/M–O(1a)	1.90064(2)	1.89989(2)	1.90101(1)
Cu(1)/M–O(1b)	1.996(6)	2.006(5)	2.004(4)
Cu(1)/M–O(2)	1.8491(35)	1.8416(27)	1.8532(24)
Cu(2)–O(2)	2.205(4)	2.2073(30)	2.2040(27)
Cu(2)–O(3)	1.9163(4)	1.91595(29)	1.91753(25)
O(2)–Cu(2)–O(3)	97.32(8)	97.42(7)	97.53(6)
O(3)–Cu(2)–O(3)	165.35(17)	165.15(13)	164.95(11)
O(3)–Cu(2)–O(3)	89.069(21)	89.044(17)	89.017(15)

Table 4
The relevant distances and superconducting T_c for the optimally doped $CuBa_2YCu_2O_7$, $Cu_{0.8}W_{0.2}Sr_2YCu_2O_{7.3}$ and $HgBa_2CaCu_2O_6$.

	$CuBa_2YCu_2O_7$	$Cu_{0.8}W_{0.2}Sr_2YCu_2O_{7.3}$	$HgBa_2CaCu_2O_6$
c (Å)	11.680	11.497	12.660
d(intra) (Å)	3.373	3.399	3.382
d(inter) (Å)	8.307	8.098	9.518
d(block) (Å)	3.700	3.683	3.919
d(apical) (Å)	2.303	2.207	2.799
T_c (K)	93	77	128

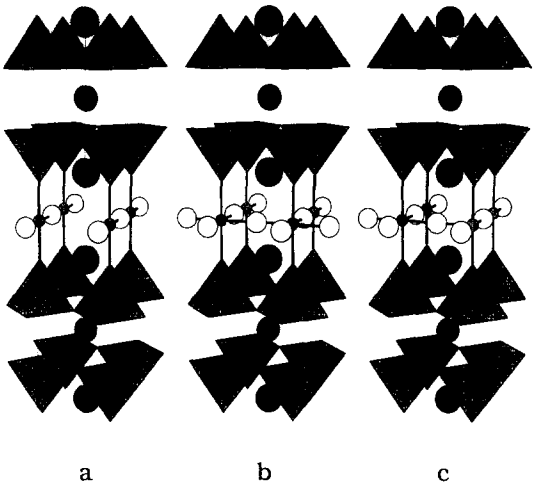

Fig. 3. (a) Model defect structures for 123, (b) dimers of corner shared Mo and W octahedra, and (c) isolated Re octahedra.

measurements were done with slow heating and cooling rates (0.6°/min) using ~ 1 g of powder. Five consecutive runs were performed without removing the specimen from the TGA apparatus using 1, 0.1, 0.01 and 0.001 atm. of oxygen, followed by the hydrogen reduction. The TGA data was obtained on cooling after a 5 h equilibrations at 950 or 850°C

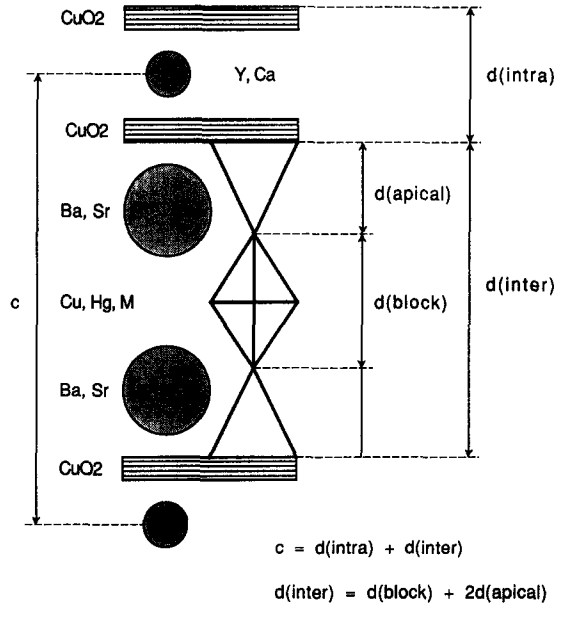

Fig. 4. Schematic structure of 1212 compounds with two-CuO_2-planes and a single metal-oxygen layer in the intermediate region.

Table 5
Oxygen content, z, and relative change in oxygen content between two consecutive annealings for $Cu_{0.8}W_{0.2}Sr_2YCu_2O_z$ determined from TGA measurements for several oxygen pressures.

Oxygen pressure (atm)	Oxygen content	Relative change in oxygen content
220	7.14	
		0.02
1	7.12	
		0.08
0.1	7.04	
		0.06
0.01	6.98	
		0.07
0.001	6.91	

for several oxygen pressures and a hydrogen reduction at 1100°C. Assuming a full reduction in hydrogen to the copper metal, SrO, Y_2O_3 and WO_2, the total oxygen content of the starting material is 7.14(2). The oxygen contents obtained after slow cooling in other oxygen pressures are shown in Table 5. Since the tungsten dioxide may show oxygen nonstoichiometry, the absolute values for the oxygen content may differ from shown in Table 5. This may explain the discrepancy observed for the oxygen contents determined from TGA and neutron diffraction (7.30) for the sample annealed at high oxygen pressure.

The relative changes in the oxygen content between consecutive TGA runs for samples slowly cooled in 220, 1, 0.1, 0.01 and 0.001 atm. of oxygen are 0.02, 0.08, 0.06, 0.07, respectively. These values do not depend on a final decomposition product after hydrogen reduction. The small relative change in the oxygen content for sample annealed at high oxygen pressure indicates that an anneal in pure oxygen is almost as effective as an anneal at 220 atm O_2, thus, the anneals at even higher oxygen pressures will not increase considerably the oxygen content or T_c. To achieve higher hole doping of the CuO_2 planes, other methods should be used, for example, Ca^{2+} substitution for Y^{3+}. The small relative change in the oxygen content at high oxygen pressure supports a model of stable complex-defects consisting of substituted metal ions and oxygen.

The high temperature TGA data show that the oxygen content remains relatively high at elevated temperatures and reduced oxygen pressure, for example, $z \sim 6.75$, even at 850 C in 0.001 atm. of oxygen. This indicates a considerably improved thermal stability of the intermediate "chain" region of the structure. The presence of the transition elements in the "chain" region decreases substantially the oxygen nonstoichiometry when compared to Y123. The Sr based 1212 materials show improved thermal stability over Y123.

3.3. Superconducting properties

To study the superconducting properties, the ac susceptibility (χ) and dc magnetization (M) were measured from 5 to 80 K in applied field from 0 to 7 T. Solid pieces as well as powdered samples with masses of about 100 mg were used for both measurements. The susceptibility was measured upon warming from a zero-field-cooled (ZFC) state using an ac field of 1 Oe at 200 Hz. The ac field was large enough to separate the grain and intergrain components, which were clearly observed for solid samples. The real part of χ close to the superconducting transition at several applied fields is shown in Fig. 5 for a powdered $Cu_{0.8}W_{0.2}Sr_2Y_{0.9}Ca_{0.1}Cu_2O_z$ sample. The transitions onsets, T_{c0}, are marked by arrows for 0 and 3 T applied field. The onset temperatures decrease slowly with increasing magnetic field, resembling behavior similar to that of the upper critical field rather than the fast decrease usually seen for the irreversibility field. The solid horizontal line denotes points at which χ' reaches 3% of the diamagnetic signal observed at 5 K and zero applied magnetic field. The temperature at which χ' reaches 3%, T_c (3%), of a signal observed at 5 K is close to the temperature at which the resistivity attains a zero value. Thus, the 3% value was conveniently chosen to compare irreversibility lines obtained from the susceptibility and magnetization measurements. These T_c (3%) values are easy to measure and can serve as a fast characterization method of intrinsic irreversibility fields for different samples of the same or similar compounds. Fig. 5 shows that T_c (3%) decreases much faster than T_{c0} with the increase of the magnetic field. The characteristic field B_c (3%) obtained from similar plots for several $Cu_{1-x}M_xSr_2Y_{1-y}Ca_yCu_2O_z$ compounds is shown in Fig. 6 as a function of temperature. The highest B_c (3%) field was observed for the $Cu_{0.8}W_{0.2}Sr_2Y_{0.9}Ca_{0.1}Cu_2O_z$ sample.

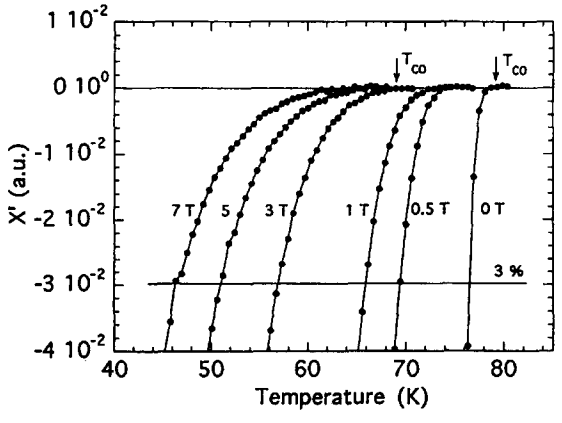

Fig. 5. Real part of the ac susceptibility close to the superconducting transition temperature at several applied fields for the $Cu_{0.8}W_{0.2}Sr_2Y_{0.9}Ca_{0.1}Cu_2O_z$ sample.

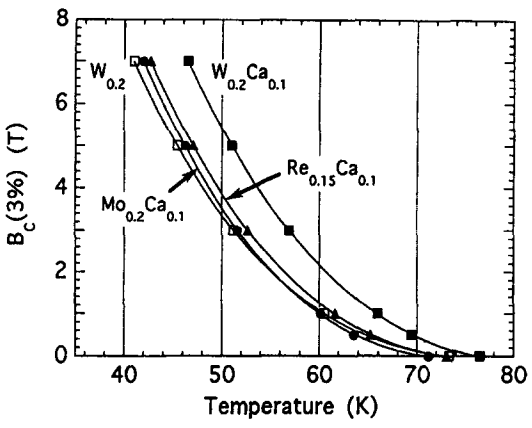

Fig. 6. Characteristic field B_c (3%) for several $Cu_{1-x}M_xSr_2Y_{1-y}Ca_yCu_2O_z$ compounds.

The volume fraction of the superconducting grains was estimated from the ac susceptibility measurements. The density of solid pieces was about 4.7 g/cm^3 (80% of the X-ray density, 5.9 g/cm^3). After the correction for demagnetizing factors, the χ was nominally equal to $-1/4\Pi$ (perfect shielding) at 5 K and zero dc field. For powdered samples and by taking a density of 5.9 g/cm^3, χ was $\sim -1/10\Pi$. For measurements on solid pieces performed in large

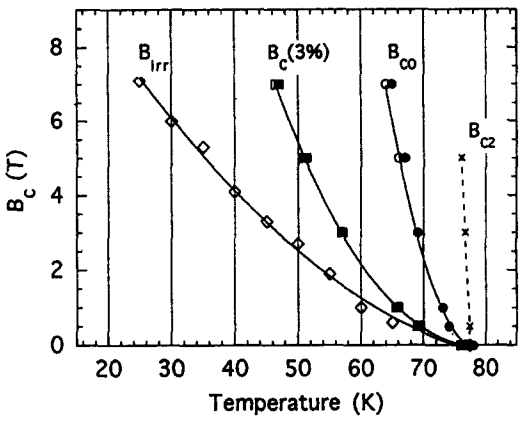

Fig. 7. Critical fields B_{c2}, B_{c0}, B_c (3%) and B_{irr} for a $Cu_{0.8}W_{0.2}Sr_2Y_{0.9}Ca_{0.1}Cu_2O_z$ sample; powders (open symbols) and solid chunks (closed symbols). B_{c2} and B_{irr} were obtained from dc magnetization, and B_{c0} and B_c (3%) from ac susceptibility.

magnetic fields, higher than 1 T, which decoupled the superconducting grains, susceptibility was also approximately $-1/10\Pi$, i.e., it was equal to χ obtained for powder samples at zero dc field. Taking into consideration the effect of the magnetic penetration depth, $\lambda \sim 0.2$ μm, which is about 30 times smaller than the grain diameter, we conclude that the volume fraction of the superconducting grains is above 50%. This relatively high volume fraction demonstrates the good quality of these granular samples compared to (Bi,Pb)2223, ~20%, [18] and Y123, ~70% [19].

The dc magnetization measurements were performed as a function of applied field at constant temperature, and as a function of temperature at constant field to determine the irreversibility field (B_{irr}) and the upper critical field (B_{c2}). All measured critical fields are shown on Fig. 7 for the $Cu_{0.8}W_{0.2}Sr_2Y_{0.9}Ca_{0.1}Cu_2O_z$ sample. The large differences observed for B_{c2}, B_{c0}, B_c (3%) and B_{irr} are similar to those observed for other high temperature superconductors. Large differences measured for the irreversibility fields B_{c0} and B_{irr} indicate a substantial influence of thermally activated processes on weak pinning. A rather weak pinning was also evidenced by observation of a sharp peak in $M(B)$ curves above the first penetration field at temperatures as low as 30 K. Moreover, the histeresis loops above 10 K have asymmetric shapes with respect to the $M = 0$ line, which indicates a strong influence of the reversible magnetization and suggests rather poor critical state parameters. Compared to that for the Bi2212 and Bi2223 compounds, the irreversibility line is at much higher temperatures and is similar to that observed for $HgBa_2CuO_4$ [20]. When the reduced irreversibility temperature, T_{irr}/T_c, is considered for several isostructural compounds, the doped $CuSr_2YCu_2O_7$ compounds have $T_{irr}/T_c = 0.85$–0.90 at 0.5 T. This reduced irreversibility temperature is higher than for $HgBa_2CaCu_2O_6$, $T_{irr}/T_c = 0.78$, similar to chemically substituted $HgBaSrCaCu_2O_6$, and smaller than the chemically substituted $HgSr_2CaCu_2O_6$, $T_{irr}/T_c = 0.96$, and Y123, $T_{irr}/T_c = 0.98$ [21]. Among these compounds, the thickness of the intermediate region between the double CuO_2 planes is smallest for $CuSr_2YCu_2O_7$. Since it is believed that the distance between the Josephson coupled superconducting CuO_2 planes is crucial for pinning the flux vortices [20] one would expect to measure the highest reduced irreversibility fields for stabilized $CuSr_2YCu_2O_7$ compounds. For an external field applied perpendicular to the a–b plane and a transport current flowing parallel, the thickness of the blocking layer is important because the flux motion at higher temperatures results from the thermally activated transition from three dimensional vortex lines to two dimensional decoupled pancake-like vortices in the CuO_2 planes [22]. For other field and current configurations, usually found for polycrystalline samples, the screening and transport currents have to cross the blocking layers and therefore the Josephson coupling energy should influence the superconducting critical properties even more effectively. Our results show that physical properties of the blocking layer in addition to its thickness determine the effective Josephson coupling between superconducting CuO_2 planes. The extrinsic bulk pinning, caused by, for example, twin boundaries, dislocations or impurities, is also very important and can be the reason for better irreversibility properties observed for Y123 and substituted $HgSr_2CaCu_2O_6$ compounds. One should also consider possible differences in the measured irreversibility fields resulting from different measurement techniques, for example, different time scales of the measurements [23].

The magnetization loops were measured at constant temperatures for powdered samples to determine the critical persistent-current density, j_p, by

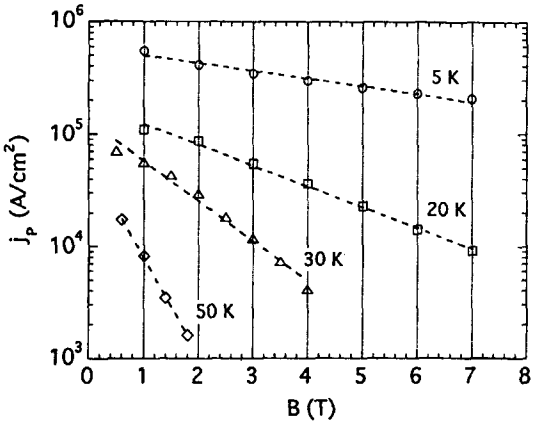

Fig. 8. Critical current determined from magnetization loops by applying the Bean formula for the $Cu_{0.8}W_{0.2}Sr_2Y_{0.9}Ca_{0.1}Cu_2O_z$ sample at 5, 20, 30 and 50 K.

applying the Bean formula, $j_p(A/cm^2) = k\Delta M/d$ (M[emu/cm^3], d[cm]). The grain diameter was used as a scaling length because the samples showed granular behavior in ac measurements. Granular behavior was evidenced by the observation that the absolute value of the real part of the ac susceptibility was several times smaller at bias fields of 1 T than at zero field and did not depend significantly on the magnitude of the field above 1 T. Moreover, the imaginary part of the susceptibility for powders did not show two maxima, which would indicate the presence of intragrain and intergrain transitions, as was observed for solid-piece samples at zero or low bias fields. Therefore, we can estimate that the intergrain coupling current is negligibly small at fields above 1 T.

We have determined the j_p as a function of applied field assuming a more spherical ($k = 40$) than plate shape of the grains, and taking $d = 6\mu$m as an average grain diameter based on SEM measurements. Fig. 8 shows the critical current for the $Cu_{0.8}W_{0.2}Sr_2Y_{0.9}Ca_{0.1}Cu_2O_z$ sample at 5, 20, 30 and 50 K. At 5 K the calculation gives $j_p \sim 5 \times 10^5$ A/cm^2 and 2×10^5 A/cm^2 for 1 and 7 T fields, respectively, showing weak dependence on the applied field. However, j_p drops more rapidly with increasing magnetic field at elevated temperatures. Therefore, the values of j_p observed below 30 K may be of interest for high field applications.

4. Conclusions

We have optimized compositions and synthesis conditions for chemically stabilized $CuSr_2YCu_2O_z$ materials with the highest T_c. The highest T_c (~ 77 K), irreversibility field, and critical current density are achieved for the Ca-doped $Cu_{0.8}W_{0.2}Sr_2YCu_2O_z$ sample. Similar optimization of superconducting properties for $CuSrBaYCu_2O_z$ and $CuBa_2YCu_2O_z$ compositions should produce considerably improved materials. Structural and superconducting properties indicate that physical properties of the intermediate region in addition to its thickness determine the effective Josephson coupling between the superconducting CuO_2 planes and that it is possible to influence the Josephson coupling by the proper choice of substituted metallic ions, formation of complex defects and by modifying the oxygen content.

Acknowledgments

This work was supported by the National Science Foundation Science and Technology Center for Superconductivity under grant No. DMR 91-20000 (BD, KR, JWK, KRP) and the U.S. Department of Energy, BES – Materials Sciences under contract No. W-31-109-ENG-38 (JDJ).

References

[1] B. Okai, Jpn. J. Appl. Phys. 29 (1990) L2180.
[2] M.R. Chandrachood, P.K. Narwnkar, D.E. Morris and A.P.B. Sinha, Physica C 194 (1992) 205.
[3] H. Shaked, P.M. Kane, J.C. Rodriguez, F.F. Owen, R.L. Hitterman and J.D. Jorgensen, Crystal Structures of the High-T_c Superconducting Copper-Oxides, (Elsevier Science, Amsterdam, 1994).
[4] S.A. Sunshine, L.F. Schneemeyer, T. Siegrist, D.C. Douglass, J.V. Waszczak, R.J. Cava, E.M. Gyorgy and D.W. Murphy, Chem. Mater. 1 (1989) 331.
[5] T. Den and T. Kobayashi, Physica C 196 (1992) 141.
[6] J.D. Jorgensen, Physics Today (June 1991) p. 34.
[7] T.P. Beales, C. Dineen, S.R. Hall, M.R. Harrison and J.M. Parberry, Physica C 207 (1993) 1.
[8] B. Dabrowski, V. Zhang-McCoy, R. Hannon, B.A. Hunter, J.D. Jorgensen and R.L. Hitterman, Physica C 208 (1993) 183.

[9] M. Vybornov, W. Perthold, H. Michnor, T. Holubar, G. Hilscher, P. Rogl, P. Fischer and M. Divis, Phys. Rev. B 52 (1995) 1389.
[10] B. Dabrowski, P. Radaelli, D.G. Hinks, A.W. Mitchell, J.T. Vaughey, D.A. Gronke and K.R. Poeppelmeier, Physica C 193 (1992) 63.
[11] Q. Huang, R.J. Cava, A. Santoro, J.J. Krajewski and W.F. Peck, Physica C 193 (1992) 196.
[12] J.D. Jorgensen, J. Faber Jr., J.M. Carpenter, R.K. Crawford, J.R. Haumann, R.L. Hitterman, R. Kleb, G.E. Ostrowski, F.J. Rotella and T.G. Worlton, J. Appl. Cryst. 22 (1989) 321.
[13] A.C. Larson and R.B. Von Dreele, General Structure Analysis System, University of California, Berkeley (1985–1990).
[14] R.L. Harlow, G.H. Kwei, R. Suryanarayanan and M.A. Subramanian, Physica C 257 (1996) 125.
[15] P.R. Slater and C. Greaves, Physica C 180 (1991) 299.
[16] J.L. Wagner, P.G. Radaelli, D.G. Hinks, J.D. Jorgensen, J.F. Mitchell, B. Dabrowski, G.S. Knapp and M.A. Beno, Physica C 210 (1993) 447.
[17] J.D. Jorgensen, D.G. Hinks, O. Chmaissem, D.N. Argyriou, J.F. Mitchell and B. Dabrowski, in: Recent Developments in High Temperature Superconductivity, eds. J. Klamut, B.W. Veal, B. Dabrowski, P.W. Klamut and M. Kazimierski (Springler, Berlin, 1996) pp. 1–15.
[18] D.-X. Chen, Yu Mei and H.L. Luo, Physica C 167 (1990) 317.
[19] D.-X. Chen, A. Sanchez, T. Puig, L.M. Martinez and J.S. Munoz, Physica C 168 (1990) 652.
[20] U. Welp, G.W. Crabtree, J.L. Wagner, D.G. Hinks, P.G. Radaelli, J.D. Jorgensen, J.F. Mitchel and B. Dabrowski, Appl. Phys. Lett. 63 (1993) 693.
[21] J. Shimoyama, S. Hahakura, R. Kobayashi, K. Kitazawa, K. Yamafuji and K. Kishio, Physica C 235–240 (1994) 2795.
[22] D.H. Kim, K.E. Gray, R.T. Kampwirth, J.C. Smith, D.S. Richeson; T.J. Marks, J.H. Kang, J. Talvacchio and M. Eddy, Physica C 177 (1991) 431.
[23] M.C. Frischherz, F.M. Sauerzopf, H.W. Weber, M. Murakami and G.A. Emelchenko, Supercond. Sci. Technol. 8 (1995) 485.